Dynamic features within subcortical network serve as potential transdiagnostic biomarker

Abstract (199/200 words)

Identifying biomarkers for multiple mental disorders is an important issue in clinical neuroscience. However, traditional case-control neuroimaging studies with static functional connectivity may provide little utility in biomarker detection. In current study, we aimed to find biomarker across a wide range of psychiatric disorders included schizophrenia (SZ, N = 168), bipolar disorder (BD, N = 49), major depressive disorder (MDD, N = 100), obsessive-compulsive disorder (OCD, N = 56), by using resting-state fMRI and dynamic functional connectivity (FNC) approach. We mainly focused on the dynamic features within subcortical network, the key site in the pathophysiology of psychiatric disorders and important hub to mediate large-scale cortical communication. Dynamic FNCs were clustered into four states by k-mean clustering. State 4, with increased functional connectivity in subcortical network (basal ganglia and thalamus), showed significant group differences. Healthy controls (HC, N = 210) dwelled significantly longer than other patients in this state. SZ engaged longer time than OCD, BD, and MDD also have more dwell time than OCD in state 4. Finally, multi-class support vector machine based on dynamic features of subcortical network successfully classified MDD and SZ from other populations. Together, our study may provide a new robust biomarker across mental disorders.

Keywords: bipolar disorder, major depressive disorder, schizophrenia, obsessive-compulsive disorder, transdiagnostic study, dynamic functional connectivity, independent component analysis, subcortical network, basal ganglia, thalamus

Introduction

The desire to classify mental disorders in objective and precise way has its roots in classical antiquity. From Galen's typology to modern scientific approaches like ICD-11 (*International Classification of Diseases*, by WHO) and DSM-V (*Diagnostic and Statistical Manual of Mental Disorders*, by APA), but completely understanding mental illnesses can still be challenging. One problem might be, diagnosis and classification are based on subjective symptoms and visible signs, and the co-morbidity also hinder the progress to make precise clinical decisions (Goldberg, 2015; Clark et al., 2019). Thus, the idea behind precision medicine has rapidly come to psychiatry (Insel and Guthbert, 2015; Fernandes et al., 2017), which is called "*precision psychiatry*". One of the main goals of precision psychiatry is to optimize diagnosis and treatment strategies. Critical to this goal is finding the *biomarker*. Traditional paradigm for detecting biomarker in field of psychiatry is case-control design, where the case refers to specific mental disorders, while the control represents healthy participants (Lewis and Pelosi, 1990). However, biomarkers identified in case-control neuroimaging studies lack disorder specificity (Sha et al., 2018), and cannot reveal the shared or distinct patterns among different mental disorders. Instead, in order to acquire more clear classification and recognition for complex mental illnesses, the field needs a step to transition to transdiagnostic designs, that is, multiple disorders should be considered concurrently (Parkes et al., 2020).

In the current study, our main goal is to find an effective biomarker in transdiagnostic design for a range of diagnostic categories, including schizophrenia (SZ), bipolar disorder (BD), major depressive disorder (MDD), obsessive-compulsive disorder (OCD), by using resting-state functional magnetic resonance imaging (rs-fMRI). rs-fMRI can represent intrinsic architecture of neural networks and has been recognized as a powerful tool in clinical neuroscience (Fox and Greicius, 2010). More specifically, we aimed to investigate: 1) whether there will be a neural biomarker (e.g.,

network) to reveal the difference across these disorders; 2) if so, how distinct would be between any pair of psychiatric disorders on the characteristics of this biomarker.

Mounting evidence suggests that deficits underlying a group of high-order and large-scale brain networks such as default mode network (DMN), cognitive control network (CC) are critical mechanisms of mental disorders (e.g., Yan et al., 2019; Bakers et al., 2014). This pervasive "corticocentric" view reflected in a large number of studies (Bell and Shine, 2016) which focused on disruptions in neocortical networks may neglect the importance of subcortical structures. Subcortical anatomical areas (major sites: basal ganglia and thalamus) affect fundamental functions such as motivation and emotion (Panksepp, 1998). Dysfunctions in subcortical structures cause apathy, depression and psychosis (Salloway and Cummings, 1994; Koshiyama et al., 2018) and be harmful for social adaptation (Schultz et al., 2019). Indeed, subcortical network is key component in the pathophysiology of psychiatric disorders. Especially some key subcortical structures, such as basal ganglia and thalamus, play important roles in supporting large-scale network communication and integrating diverse signals from cortex (Crossley et al., 2014).

Here, we hypothesized that the subcortical network would be potential biomarker across multiple mental disorders and would treat it as our main research goal. Recently, one large-scale meta-analytic study has found the patterns of dysfunction in the subcortical system (e.g., basal ganglia, thalamus) were common across psychiatric disorders compared to healthy controls (Sha et al., 2018). Other qualified case-control studies revealed structural abnormalities within subcortical network in bipolar disorder (Hibar et al., 2016), obsessive-compulsive disorder (Kong et al., 2020), major depressive disorder (Schmaal et al., 2016), as well as schizophrenia (Gur et al., 1998). One task-based fMRI study has implicated the functional connectivity of subcortical brain regions (amygdala-striatum pathway) can distinguish depressed mood phase from manic phase in bipolar adults (Man et al., 2019). Mamah *et al*. conducted shape analysis in subcortical and found few similarities in surface deformation patterns

between schizophrenia and bipolar disorder (Mamah et al., 2019). But these case-control design studies cannot give direct evidence that whether the features of subcortical network can be different among pairs of psychiatric population under direct comparisons, and only a small number of empirical studies were in transdiagnostic approach with large-sample and multiple psychiatric disorders. Thus, this current investigation is necessary and urgent.

An increasing number of studies provided solid evidence that the brain is a dynamic system, rather than static one on a micro-time scale (Calhoun et al., 2014; Preti et al., 2017). Dynamic functional connectivity (dynamic FNC), which is implemented by the sliding window method (Liao et al., 2017; Liu et al., 2018), is an ideal approach to characterize the dynamic nature of brain (Calhoun et al., 2014). And it also be useful for detecting and predicting diseases, such as Parkinson diseases (Fiorenzato et al., 2019), schizophrenia (Damaraju et al., 2014), bipolar disorder (Rashid et al., 2014), and major depressive disorder (Wu et al., 2019). Given its importance and efficacy for characterizing diseases, a few transdiagnostic studies began to adopt this method to explore dynamic FNC characteristics among large-scale brain networks (Reinen et al., 2018; Li et al., 2020). But these studies had relatively small sample sizes or studied limited diseases (i.e., SZ and BD or SZ, MDD and BD).

Here, we configure our transdiagnostic design with sliding-window approach (Allen et al., 2014; Calhoun et al., 2014) to portray the features of dynamic functional connectivity within subcortical network among a range of psychiatric disorders including BD (n=49), MDD (n=100), OCD (n=56), SZ (n=168), and healthy controls (n=210). We first compared the temporal properties between healthy and clinical populations and then conducted pair-wise comparisons among all kinds of mental illnesses. To exclude the possibility that some results might be attributed to treatment effects, the current study only recruited medication-naïve individuals suffering from four psychiatric disorders. Of note, all participants' data were collected by the same scanner and acquisition sequence to ensure the data comparability.

Method

Ethic approval.

The current study was carried out in accordance with principles of the Declaration of Helsinki and approved by a local Research Ethics Committee of the Second Affiliated Hospital of Xinxiang Medical University (Xinxiang, China). All participants provided written informed consent after the experimental procedure had been fully explained and were informed of their right to withdraw at any time during the study.

Participants.

We collected resting-state functional magnetic resonance imaging (fMRI) data from 583 individuals, including 210 healthy controls (HC, free of current or a history of psychiatric disorders) and 373 patients who were diagnosed with bipolar disorder (BD, $N = 49$), major depressive disorder (MDD, $N = 100$), obsessive compulsive disorder (OCD, $N = 56$), or schizophrenia (SZ, $N = 168$). All participants were screened using non-structured interviews based on the diagnostic criteria of the DSM-IV by experienced psychiatrists from the Second Affiliated Hospital of Xinxiang Medical University (Xinxiang, China). Thirty-eight participants (MDD = 2, OCD = 4, SZ = 26, HC = 6) were excluded from the subsequent analyses due to significant head motion (above 2.5 mm or 2.5° in any directions, see *Data preprocessing* for more details). Thus, data from 545 participants were included in the formal data analysis: 49 with BD, 98 with MDD, 52 with OCD, 142 with SZ, and 204 HCs. Demographics information and clinical characteristics of included participants ($N = 545$) were shown in Table S1.

Neuropsychological and neuropsychiatric assessment.

We asked participants to complete questionnaires to assess related symptoms of each disorder. Psychiatry symptoms of SZ patients were obtained using the Positive and Negative Syndrome Scale (PANSS) (Kim et al., 2012). BD and MDD patients completed the Beck Anxiety Inventory (BAI) (Beck et al., 1988) and Beck Depression Inventory (BDI) (Beck et al., 1961) assess their affective symptoms. The Yale-Brown Obsessive-Compulsive Scale (Y-BOCS) (Goodman et al., 1989) was employed to

assess the obsessive thoughts and compulsive behaviors of OCD patients. We calculated the total scores of each questionnaire and reported them in Table S1.

Image acquisition.

Functional brain images were acquired using a 3-Tesla Siemens Trio scanner at the Second Affiliated Hospital of Xinxiang Medical University (Xinxiang, China). Blood oxygen level-dependent (BOLD) gradient echo planar images (EPIs) were obtained using a 12-channel head coil [64 × 64 × 33 matrix, voxel size = 3.44 × 3.44 × 4 mm^3, repetition time (TR) = 2000 ms, echo time (TE) = 30 ms, flip angle = 70°, field of view (FOV)=256 × 256mm^2]. A high-resolution T1-weighted structural image was subsequently acquired (256 × 256 × 144 matrix with a spatial resolution of 1 × 1 × 1 mm, TR = 2530 ms, TE = 3.37 ms, inversion time (TI) = 1100 ms, flip angle = 70°).

Data analysis.

Data preprocessing. The fMRI data was preprocessed using SPM12 (Wellcome Trust Centre for Neuroimaging, London). Similar to previous studies (Hampson et al., 2002; Long et al., 2008), the first 10 functional images were discarded to avoid initial steady-state problems. Remaining images were spatially realigned for head motion correction, and corrected for slice acquisition temporal delay. Functional images were then co-registered to each participant's segmented gray matter T1-weighted image, spatially normalized to a common the Montreal Neurological Institute (MNI) space, and resampled into 3 × 3 × 3 mm^3 voxels. Finally, all functional images were spatially smoothed with an isotropic 4mm FWHM Gaussian kernel.

Group independent component analysis (ICA). ICA provides a blind and objective separation of spatially independent components with potential temporal correlations. Here we decomposed all preprocessed data into functional components of unique time course profiles, using group ICA implemented in the GIFT toolbox (http://mialab.mrn.org/software/gift/) (Calhoun et al., 2001a). First, we performed a subject-specific principal component analysis (PCA) for data reduction. Similar to

previous study (Rashid et al., 2016; Allen et al., 2014), 120 principal components were remained for each participant. Then at a group level, we employed the expectation-maximization (EM) algorithm (Roweis, 1998) in the GIFT toolbox to decompose the resting-state data into 100 group independent components (Abou-Elseoud et al., 2010), we repeated the Infomax ICA algorithm (Bell and Sejnowski, 1995) for 20 times in ICASSO (Himberg et al., 2004) to ensure the reliability and stability. Subject-specific spatial maps and time-courses were then estimated by the back-reconstruction approach (Calhoun et al., 2001b). We then identified 50 meaningful independent components from the 100 group independent components based on the following criteria (Allen et al., 2014; Rashid et al., 2016): 1) whether the peak activation coordinates of the functional components were primarily located in grey matter; 2) whether the component showed low spatial overlap with white matter structures, vascular, ventricular, edge regions corresponding to artifacts. In these remaining components, 38 were cortical, 5 were cerebellar. We identified seven components (Figure 1A and Figure S1) that were localized in thalamus and basal ganglia. These seven components were subsequently used to construct subcortical network based on the templates provided in previous research (Ystad et al., 2010; Allen et al., 2014). Then the time-courses of the seven components were detrended, despiked and low-pass filtered with a high-frequency cutoff of 0.15 Hz to remove remaining noise sources (Allen et al., 2014). We also regressed out the six parameters of head movement.

Dynamic functional connectivity. We employed a sliding temporal window approach to examine dynamic functional connectivity (FNC) of the resting-state data. This analysis was conducted by the dynamic FNC network toolbox in GIFT. In line with previous work (Shirer et al., 2012; Allen et al., 2014), the time-course of each independent component was divided into 200 windows, with each window of width = 30 TR and sliding step = 1 TR. We estimated covariance using the regularized inverse covariance matrix (Varoquaux et al., 2010; Smith et al., 2011) to avoid noise caused by covariance estimation using time series of shorter length. In addition, a L1 norm

constraint on the inverse covariance matrix was applied to enforce sparsity in the graphic LASSO framework (Friedman et al., 2008).

Clustering analysis. A *k*-means clustering algorithm (Lloyd, 1982) was applied on windowed FNC matrices to identify the reoccurring FNC patterns (i.e., FNC states) across participants. The Manhattan distance matric, shown to improve the effectiveness of *k*-means clustering algorithm for high-dimensional data (Aggarwal et al., 2001), was applied to assess the similarity between different windows of FNC. A cluster validity analysis (i.e., the elbow method, Allen et al., 2014) was then conducted on the exemplars of all participants to obtain the optimal number of clusters. All clustering analyses were iterated 5 times in GIFT to produce reliable results. As a result, we determined four clusters ($k = 4$) as the optimal number of clusters.

State analysis and Graph theory analysis. For each state, we calculated the mean dwell time (i.e., the number of consecutive windows belonging to the same state) and frequency (i.e., the number of windows of each one state). We also calculated the total number of transitions from one state to a different state. The mean dwell time, frequency, and the number of transitions reflect the temporal properties of the dynamic FNC states. Moreover, we extracted the FNC strength within the subcortical network for each window and averaged the FNC strength across the windows belonging to the same state to index the FNC strength of each state.

Graph metrics for the FNC of each state were also calculated for further understanding. We calculated global efficiency and local efficiency by using the graph theoretical network analysis toolbox implemented in the Brain Connectivity Toolbox (Rubinov and Sporns, 2010). These two indices can be used to elucidate the information flows efficiency at global and local level. Higher network efficiency (globally and locally) indicated stronger information processing ability (Rubinov and Sporns, 2010; Latora and Marchiori, 2001). Technically, global efficiency was computed as the average inverse shortest path length in the network (i.e., in the

binary matrix which had been defined from subcortical network), and local efficiency was estimated as the global efficiency calculated on node neighborhoods (Latora and Marchiori, 2001).

Moreover, given that the matrices of each state were thresholded repeatedly, we calculated the area under the curve (AUC) for each state to index a threshold-independent assessment for the topological property of the networks.

For each index mentioned above, we first performed one-way analysis of covariance (ANCOVA), with Group (HC vs. patients) as factor, and with age, gender and education as covariates to investigate the general main difference between patients and healthy controls. Then we aimed to estimate the group difference among the four kinds of psychiatric patients with ANCOVA (with age, gender and education as covariates). To further reveal the distinct or shared results pattern between specific patient groups, we subsequently conducted *Post hoc* analyses. Multiple comparisons were corrected by false-discovery rate (FDR, $p < 0.05$).

Network-based statistics. To further anchor the specific pairs of brain regions wherein functional connectivity within subcortical network showed difference between healthy control and patients, as well as among all mental disorders, we adopted network-based statistic (NBS) approach (Zalesky et al., 2010; t-threshold: $t > 3.1$; permutation: 5000 randomizations). The purpose of the NBS here is to identify any potential connected structures that are significantly different between any pairs of groups. For each participant, an $N \times N$ connectivity matrix was constructed in the same way mentioned above. Then the matrix was transformed to $N\,(N - 1)/2$ unique pairwise associations, and the test statistics calculated independently adopting the values stored in each cell of the matrix.

Classification analysis based on dynamic FNC. To classify different psychiatric disorders, we conducted classification analysis using the dynamic FNC matrix (Rashid et al., 2016). We built a regression matrix of 4 disorder groups (i.e., BD, MDD, OCD, and SZ) and four states (derived from the dynamic FNC clustering

analysis). We then regressed out the windowed FNC matrices at each time window using the regression matrix. This analysis thus resulted in 16 β coefficients for each time window for each participant. We averaged β coefficients across all time windows and saved 16 mean β coefficients for each participant, serving as the dynamic FNC features for further classification analysis. For the dynamic FNC features-based classification, we employed a supervised machine learning method, i.e., multi-class support vector machine (R, e1071 package; Meyer et al., 2014). We used a standard 10-fold cross-validation to estimate the generalization error of the classifier. The data was randomly divided into 10 subgroups, 9 of which was used to train classifier to predict the left one subgroup, and this procedure was repeated for 10 times. The classification accuracy was calculated by using the correctly classified label dividing by total number of the sample.

Results

Subcortical network and its functional connectivity in four states.

Spatial map of subcortical network identified using the group independent component analysis was shown in Figure 1A. Independent components were grouped in subcortical network based on their anatomical and presumed functional properties: subcortical network (components: 2, 20, 55, 59, 69, 71, 94). And our subcortical network was mainly formed by basal ganglia (BG) and thalamus (Figure S1), which are recognized as the critical elements in subcortical structure (Salloway and Cummings, 1994; Bell and Shine, 2016). We adopted a k-means clustering algorithm to cluster dynamic FNC from all subjects into four distinct connectivity states. Figure 1B shows the cluster centroid and the percentage of occurrences of each state (arranged in the order of emergence). These matrices reflect the functional connectivity within subcortical network.

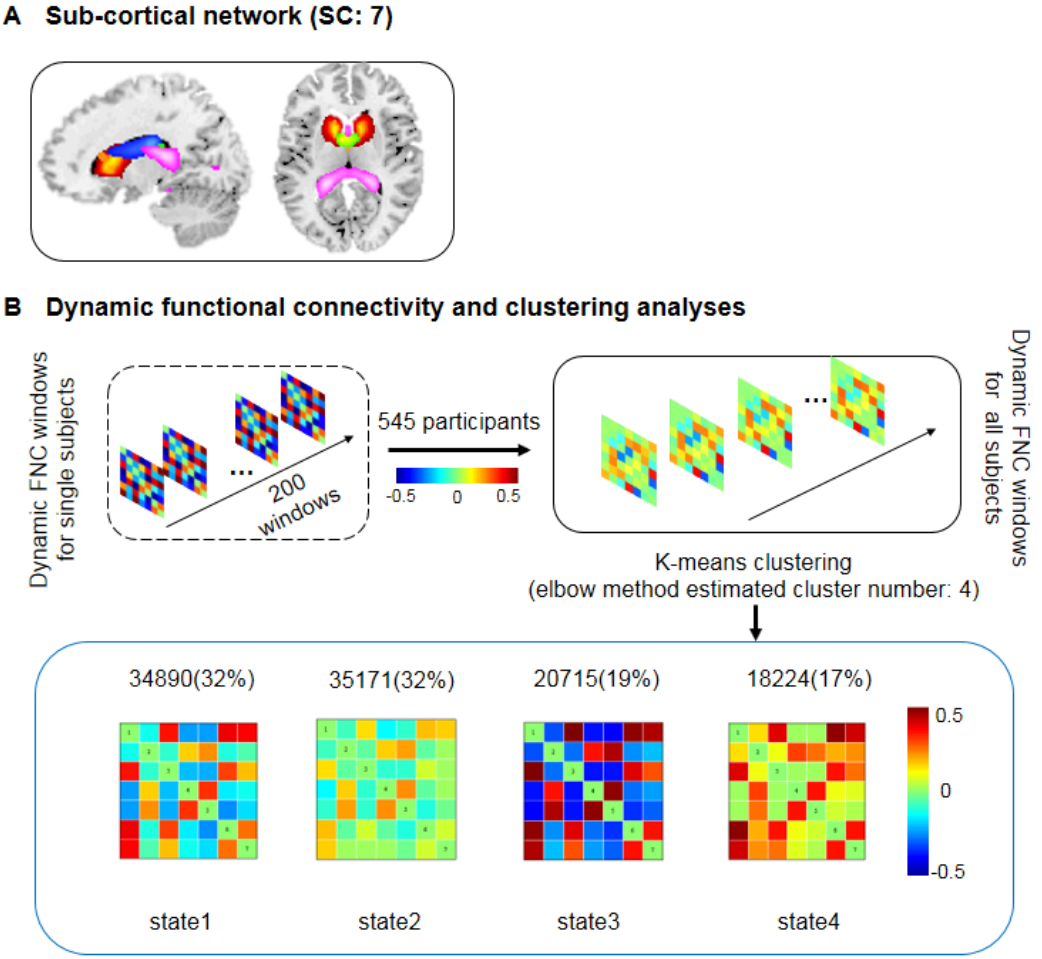

Figure 1. Composite map of the subcortical network. And the pipeline of dynamic functional connectivity and clustering analyses.

(A) The subcortical network (SC, including 7 components) was derived from group spatial independent components analyses among all participants. (B) First, for each participant, the dynamic functional connectivity (dynamic FNC) matrices are estimated on each sliding window (200 windows) of a set of components within the subcortical network. Then we applied k-means clustering algorithm on the dynamic FNC matrices across all subjects to assess the reoccurring FNC's states. Optimal number of states was determined by elbow method. We showed the averaged FNC pattern and the corresponding total number of windows in each state, percentage of each occurrences was presented in parentheses. The color bar represents the z value of FNC.

Different temporal properties between healthy control and patients in subcortical network

We first compared the mean dwell time between healthy control (HC) and all patients

(i.e., BD, MDD, OCD and SZ) in each state (Figure 2). Using one-way analysis of covariance (ANCOVA), with Group (HC vs. patients) as factor, and with age, gender and education as covariates, we found that the patients had higher mean dwell time than healthy controls in state 1 (patients: 62.868 ± 39.949 vs. healthy controls: 55.289 ± 40.120; $F(1,500)=4.814$, $p = 0.029$, $\eta^2 =0.010$) and state 2 (patients: 66.642 ± 56.247 vs. healthy controls: 53.897 ± 57.016; $F(1,500)=9.778$, $p = 0.002$, $\eta^2 =0.019$). In state4, the heathy controls (41.455 ± 58.477) showed significant higher mean dwell time than patients (26.466 ± 40.703; $F(1,500)=18.121$, $p < 0.001$, $\eta^2 =0.035$). No significant difference was found in state 3 ($F(1,500)=1.333$, $p = 0.249$, $\eta^2 = 0.003$). We did not observe significant difference on the number of transitions between healthy controls and patients ($F(1,500)=0.158$, $p = 0.691$, $\eta^2 < 0.001$). Multiple comparisons were corrected by false-discovery rate (FDR), $p < 0.05$. All contrasts remained the same after FDR correction. Results on fraction of time was similar with the mean dwell time (see Table S2).

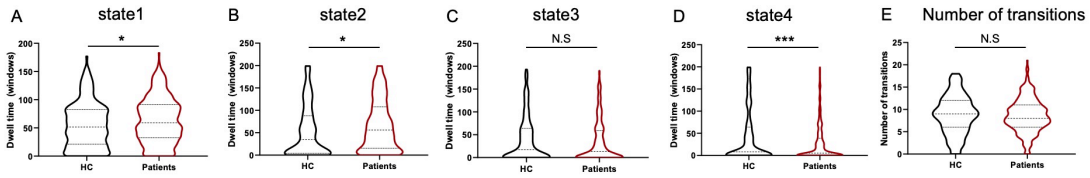

Figure 2. Mean dwell time of dynamic FNC states and number of transitions between healthy control and patients. (A, B) In state1 and state2, patients engaged more time than healthy control did. (C) In state3, no difference was found between healthy control and patients. (D) In state4, patients engaged less time than healthy control did. (E) No significant difference on number of transitions between healthy control and patients. Multiple comparisons were corrected by FDR, $p < 0.05$. All analyses reported controlled age, gender and education. (Error bars represent standard error. p<0.05*, N.S, not significant). HC, healthy controls;

Distinct temporal properties among patients in subcortical network in state 4. Next, we aimed to investigated which dynamic FNC state would show distinct temporal properties among the four groups of patients (Figure 3). The follow-up

analyses by adopting one-way analysis of covariance (ANCOVA), with Group (BD vs. MDD vs. OCD vs. SZ) as factor, and with age, gender and education as covariates on mean dwell time showed significant main effect of Group in state 4 ($F(1,304)=5.937$, $p = 0.001$, $\eta^2 = 0.056$). *Post hoc* analyses revealed that the SZ were associated with higher dwell time than BD (SZ vs. BD, $F(1,162)=9.820$, $p = 0.002$, $\eta^2 = 0.059$) and OCD (SZ vs. OCD: $F(1,165)=12.847$, $p < 0.001$, $\eta^2 = 0.074$), and MDD patients showed more dwell time than OCD patients ($F(1,141)=9.335$, $p = 0.003$, $\eta^2 = 0.064$). No differences were found between BD and MDD ($F(1,138)=0.900$, $p = 0.344$, $\eta^2 = 0.007$), neither for BD and OCD ($F(1,92)=1.544$, $p = 0.217$, $\eta^2 = 0.017$), SZ and MDD ($F(1,211)=2.491$, $p = 0.116$, $\eta^2 = 0.012$). Interestingly, we also observed significant main effect of Group on the number of transitions ($F(1,304)=5.484$, $p = 0.001$, $\eta^2 = 0.052$). *Post hoc* analyses revealed that the BD patients had higher number of transitions than MDD ($F(1,138)=10.549$, $p = 0.001$, $\eta^2 = 0.073$) and OCD ($F(1,92)=11.799$, $p = 0.001$, $\eta^2 = 0.118$), and the SZ patients also had more transitions among the four dynamic FNC states than OCD ($F(1,165)=4.769$, $p = 0.030$, $\eta^2 = 0.029$). No other contrasts showed significant differences (i.e, BD vs. SZ, SZ vs. MDD, MDD vs. OCD; all $p > 0.06$). Multiple comparisons were corrected by false-discovery rate (FDR), $p < 0.05$. All contrasts remained the same (except the comparison of SZ vs. OCD became marginally significant, $p_{corrected} = 0.06$) after FDR correction. Results on fraction of time was similar with the mean dwell time (see Table S3).

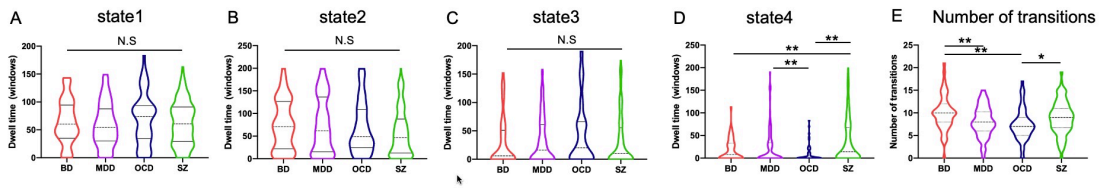

Figure 3. Mean dwell time of dynamic FNC states and number of transitions among all patients.

(A, B, C) In state1, state2, and state3, no difference was found among the four groups of patients.

(D) In state4, the main effect of Group was significant. Specifically, SZ patients engaged higher

dwell time than BD and OCD patients, MDD patients showed larger dwell time than OCD patients. No significant results were found on other contrasts. (E) The number of transitions among four groups of patients revealed significant main effect of group. BD patients showed more transitions than MDD and OCD patients, moreover, SZ patients had more transitions among the four states than OCD did. No significant results were found on other contrasts. Multiple comparisons were corrected by FDR, $p < 0.05$. All analyses reported controlled age, gender and education year. (Error bars represent standard error. $p<0.05$*, $p<0.01$**, N.S, not significant).

Exploring the meaning of in state 4

Interpreting the meaning of dynamic FNC states is essential. Consistent with previous studies, we then explored the network properties in the dynamic FNC states (Allen et al., 2014; Wu et al., 2019).

From the results mentioned above, the state 4 was the only state which showed significant difference between HC and patients, as well showed difference among the four groups of patients. We then explore the meaning of state 4. We focused on three indices which have been frequently described in previous research (Wu et al., 2019; Shi et al., 2018) including functional connectivity strength, global efficiency and local efficiency within certain brain networks. Specifically, we conducted two kinds of analyses. First, we investigated the difference between state 4 and other three states, to reveal the uniqueness of state 4 (Figure 4). Then we delineated the network properties including functional connectivity strength, global efficiency and local efficiency within subcortical network in state 4 (Figure 5), to show what exactly the difference in dwell time windows may indicate.

To make our first goal, we directly compared the differences among all states on the three interested indices. One-way analysis of covariance (ANCOVA), with Group (the four states) as factor, and with age, gender and education as covariates showed significant main effect of group on functional connectivity($F(1,126)=11.978$, $p < 0.001$, $\eta^2 = 0.222$), as well as significant main effects of group on global efficiency ($F(1,126)=4.632$, $p = 0.004$, $\eta^2 = 0.099$), but no significant main effect was found on local efficiency ($F(1,126)=1.988$, $p = 0.119$, $\eta^2 = 0.045$). We further investigated the

group differences among the four states on functional connectivity and global efficiency. *Post hoc* analyses on functional connectivity showed that the FNC and global efficiency in subcortical network in state 4 was higher than any other states (all $p < 0.001$).

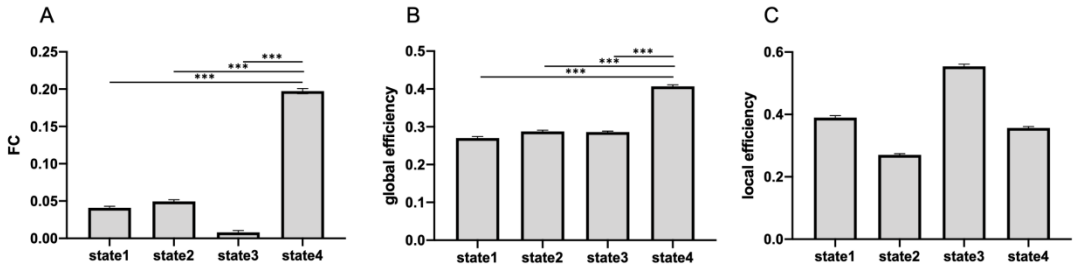

Figure 4. Uniqueness in state 4.

(A, B) Functional connectivity and global efficiency within subcortical network showed significant main effect, and the state4 was associated with higher FNC and global efficiency than other three states. (C) No main effect was found on local efficiency. (Error bars represent standard error. p<0.05*, p<0.01**, p<0.001***).

For our second purpose, we first examined the difference between HC and patients on the three indices mentioned above. One-way analysis of covariance (ANCOVA), with Group (HC vs. patients) as factor, and with age, gender and education as covariates showed significant main effect of group on functional connectivity($F(1,284)=17.872$, $p < 0.001$, $\eta^2 = 0.060$), global efficiency ($F(1,284)=8.869$, $p = 0.003$, $\eta^2 = 0.031$) and local efficiency ($F(1,284)=4.863$, $p = 0.028$, $\eta^2 = 0.017$). That the HC revealed higher functional connectivity, as well as global, local efficiency than patients. Then we investigated the group difference among the four patients. The results revealed that the main effect of Group (BD vs. MDD vs. OCD vs. SZ) in ANCOVA was significant only on functional connectivity strength ($F(3,165)=3.028$, $p=0.031$, $\eta^2 = 0.054$), neither on global nor local efficiency (all $p>0.140$). *Post hoc* analyses on functional connectivity showed marginally significant difference between BD and SZ (BD < SZ; $F(1, 67)=3.489$, $p=0.065$, $\eta^2 = 0.035$), as well as OCD and SZ (OCD < SZ; $F(1, 97)=3.639$, $p=0.060$, $\eta2 = 0.038$). The difference between MDD and OCD was

significant (MDD < OCD; $F(1,63)=7.963$, $p = 0.006$, $\eta^2 = 0.119$). Contrast between MDD and OCD remained significant after FDR correction.

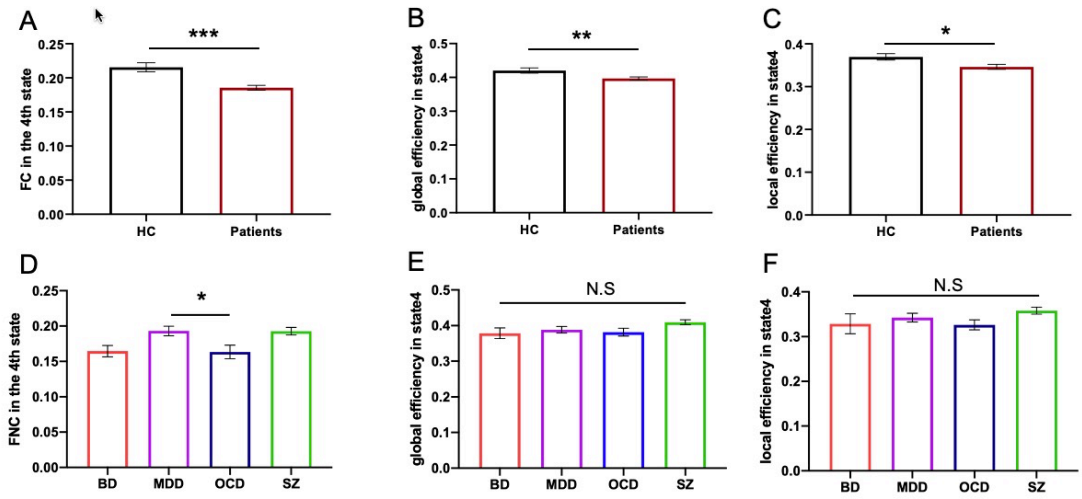

Figure 5. Network properties in state 4.

(A, B, C) Healthy controls revealed larger functional connectivity strengths, higher global and local efficiency than patients. (D) Functional connectivity among four groups of patients revealed significant main effect. (E, F) No significant main effect among the four groups on global efficiency, nor on the local efficiency. (Error bars represent standard error. $p<0.05$*, $p<0.01$**, $p<0.001$***, N.S, not significant).

Further, the network-based statistical (NBS) analysis indicated that in state 4, healthy controls revealed stronger connectivity both within basal ganglia nuclei (included caudate nucleus, ventral striatum, putamen, nucleus accumbens; these components were depicted in yellow), and between thalamus (depicted in grey here) and basal ganglia elements (Figure 6A). Similar results were also identified in SZ *vs.* BD comparisons (Figure 6B). The chord diagram presented here was created by R package *circlize* (https://github.com/jokergoo/circlize). No significant differences were detected in other pairs of comparisons.

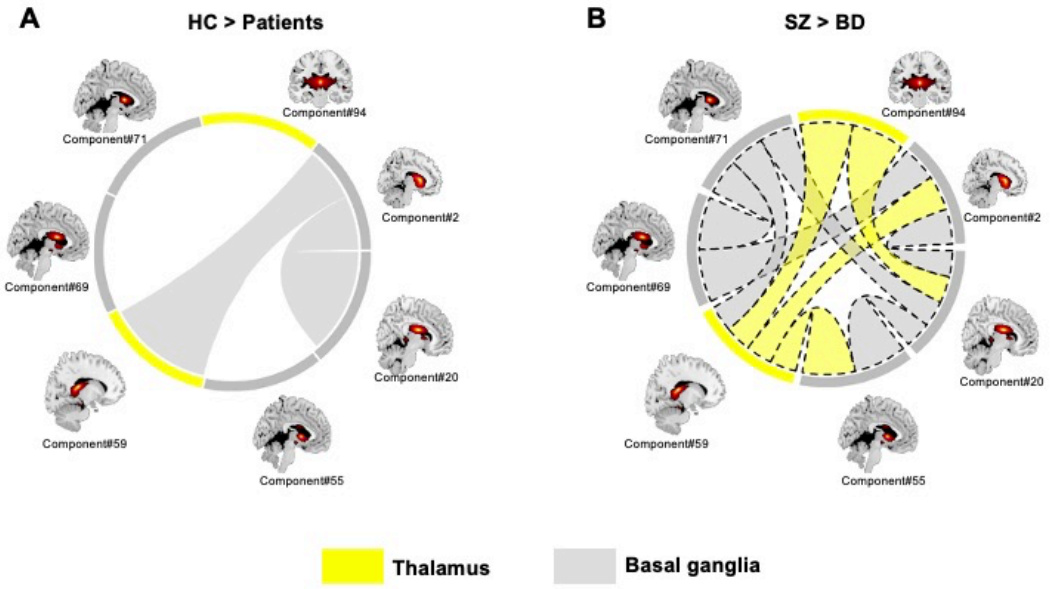

Figure 6. Results of network-based statistics in state 4.

(A) Healthy controls have stronger connections within basal ganglia nuclei, and thalamus-basal ganglia. (B) SZ patients showed more connections within thalamus, basal ganglia nuclei, as well as the stronger inter-brain communication between thalamus and basal ganglia.

Classification results based on dynamic FNC features

The multi-class SVM based on dynamic FNC approach showed classification accuracy of 22.44% for BD, 55.10% for MDD, 23.07% for OCD, and 85.92% for SZ (Figure 7B). Here, the Venn diagram were generated with R package *venneuler* (Wilkinson, 2012). The average accuracy expected due to chance is around 25%. Thus, the trained classification model generally classified MDD and SZ well.

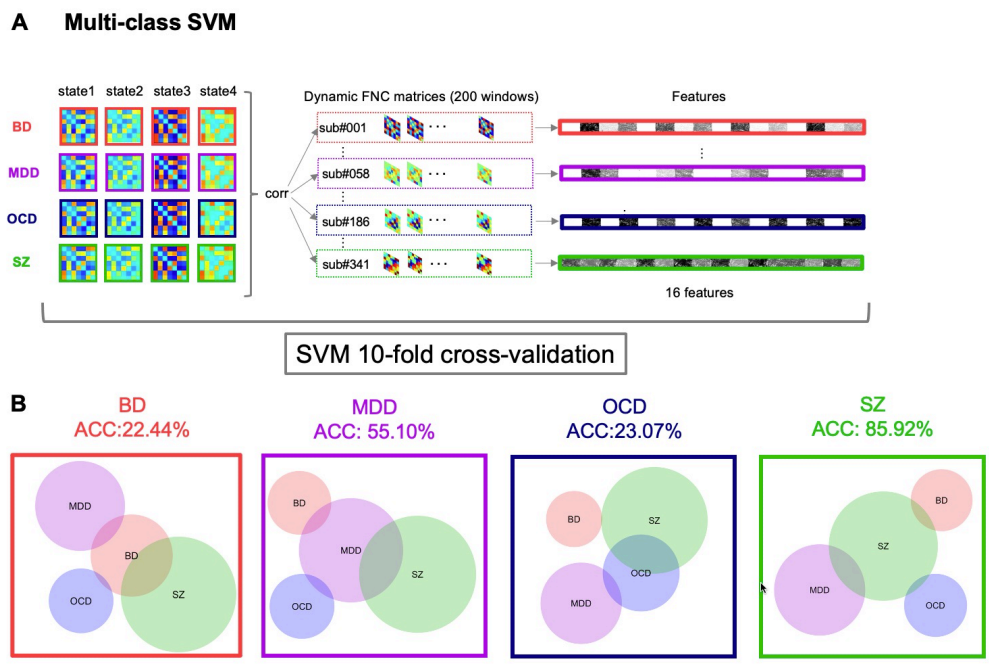

Figure 7. The pipeline of classification approach and the results of classification.

(B) An overview of classification approach for classification. We first extracted the averaged FNC pattern for each state for each patients' group, respectively. Then we performed Pearson correlation between the FNC in each window and the FNC pattern in all states among all groups. These procedures ended up with 16 averaged features for each participant.

(C) Next, we adopted the similar procedure and multi-class SVM to classify the four kinds of patients. Results showed the model performed well for classifying MDD and SZ patients (above chance level, 25%). Venn diagram revealed the how the wrong classified labels allocated at other kind of patients.

Default mode network and cognitive control networks failed to show difference among the patients.

We also investigated the whether the dynamic FNC states in default mode network (DMN) and cognitive control network (CC), which were important for mental disorders (Baker et al., 2019), would reveal difference between healthy controls and patients, as well among the patients. The DMN and CC (see Figure S2) were identified using the group independent component analysis.

Consistent with our previous analyses on subcortical network, we first examined the group difference between healthy controls and patients, then examined the group difference among the four kinds of patients. However, all states in DMN failed to show difference between HC and patients, as well as among patients (all $p > 0.07$ after FDR correction; Table S4). Likewise, the cognitive control network neither reveal distinct dynamic FNC properties between HC and patients, nor among the four groups of patients (all $p > 0.10$ after FDR correction; Table S5).

Discussion

This study adopted ICA and dynamic functional connectivity (FNC) approaches to capture the difference in subcortical network dynamic FNC features in transdiagnostic way. Using advanced clustering algorithm, we defined four reoccurring FNC states during resting-state scanning across entire populations. Wherein the state 4 exhibited significant differences, between healthy control and all mental disorders, as well as among the four groups of patients. Specifically, patients generally showed less dwell time in state 4 than healthy controls. *Post hoc* analyses identified that schizophrenia (SZ) engaged higher dwell time in state 4 than obsessive-compulsive disorder (OCD) and bipolar disorder (BD). And the major depressive disorder (MDD) revealed longer dwell time than OCD in state 4. Intriguingly, adopting multi-class support vector machine based on dynamic FNC within subcortical network generally showed ideal classification accuracy for MDD and SZ. These findings begin to delineate the dynamic properties of one of the most critical neuropsychiatric related brain networks, and open new avenues for developing potential biomarkers for a wide range of mental disorders.

Accumulating evidence suggests that basal ganglia (BG) and thalamus play a critical role in supporting the convergence of afferent information from cortical system. As detailed in the following, projections from cortical structures terminate in the striatum (key input structure of BG), then the output is channeled back to cerebral cortex via thalamus. This procedure depicted the general organization of cortico-basal ganglia-thalamic (CBG) loop, and widely affected diverse cognitive process including emotion (Pessoa, 2016) and cognitive control (Furman et al., 2011), which may form the backbone of the pathophysiology of several mental disorders. Furthermore, basal ganglia and thalamus were identified as important affected hub regions in large-scale brain networks (van den Heuvel and Sporns, 2011; McColgan et al, 2015), and served as major pathological foci in a range of psychiatric and neurological disorders (Crossley et al., 2014). In the current investigation, basal ganglia and thalamus

consisted our subcortical network. State 4 was characterized by stronger functional connectivity strength and higher global communication efficiency than other three states. Compared to healthy controls, all patients engaged relatively less dwell time in this state, as well as weak functional connectivity strength. More specifically, the network-based statistical (NBS) analysis further suggested the healthy controls had increased connection between basal ganglia and thalamus than patients did. These findings may indicate that decreased integration between basal ganglia and thalamus would be a transdiagnostic feature when compared to healthy populations.

Both SZ and BD patients have symptoms (e.g., acute mania) that overlap and share environmental risk and genetic factors (Lichtenstein et al., 2009). Distinguishing SZ from BD patients is challenging and difficult to clinicians. Interestingly, we found that SZ patients engaged more time in state 4 than BD patients. Furthermore, SZ patients revealed stronger functional connectivity strength within basal ganglia, thalamus, as well as enhanced connections between these two critical subcortical systems. Previous structure MRI study (Mamah et al., 2016) found SZ patients showed enlargement of basal ganglia than BD patients. Combing our current findings, we may infer the abnormalities in subcortical network, both in structure and function approach, could become solid biomarkers to diagnose these two types of complex mental illnesses.

A large number of studies indicated that the cortico-striatal-thalamic loop was important for understanding the underlying brain mechanisms of MDD and OCD patients (see review, Gunaydin and Kreitzer, 2016). Traditionally, the OCD patients can be characterized the dysfunction within orbitofronto (OFC)-striatal-thalamus loop. And MDD patients, who generally show reduced sensitivity to reward, which was mainly attributed to the dysfunctional dorsal lateral prefrontal cortex (dlPFC)-striatal-thalamus loop (Peters et al., 2016). One representative empirical study (Figee et al., 2011) suggests that the OCD patients also showed attenuated neural activity in basal ganglia structure (i.e., NAc) during reward anticipation. We found that MDD patients spent significantly more time in state 4 than OCD patients,

in subcortical network. Based on our current results and previous findings, we may keep cautious to infer that the different engaged time in dynamic period with higher connection strength between basal ganglia-thalamus could distinguish the potential overlap between MDD and OCD patients in negative thoughts processing (Fallucca et al., 2011), which is highly related to reward sensitivity.

Likewise, we detected significant difference between SZ and OCD patients in state 4. To our knowledge, limited research directly compared these two disorders (but see Kang et al., 2008). *Kang et al.* conducted three-dimensional shape deformation analysis on thalamic nuclei to clarify the different features between SZ and OCD patients (gender-matched, age-matched), however, they did not find significant group difference. Our current investigation, instead, classified SZ patients from OCD patients by performing dynamic FNC analysis within basal ganglia-thalamus connected network, may fill the important gap that effectively distinguishing SZ from OCD patients in clinical neuroscience.

Although we did not observe significant difference on transition numbers within subcortical network between healthy controls and patients. Some interesting results from comparisons among patients need to be briefly discussed here. BD patients switched more frequently than MDD did in subcortical between distinct states. This pattern may be consistent with the pathological mood instability and fluctuations of bipolar disorder (Geddes et al., 2013).

The current study has several notable strengths. First, a lot of previous clinical neuroimaging studies mainly focused on the deficits in large-scale cortical network but ignored the importance of subcortical regions, like the basal ganglia and thalamus, which serve as the major sites to support large-scale network integration (McColgan et al, 2015) and widely affected multiple mental disorders (Crossley et al., 2014). Thus, our findings yield unique insight into the role of subcortical structures in understanding the pathological features of psychiatric disorders. Second, we adopted transdiagnostic design with large sample and multiple mental illnesses to avoid the

potential bias and unstable conclusions in previous psychiatric studies with small samples, and traditional case-control design. Third, using advanced dynamic functional connectivity framework, we could obtain the shared and distinct instantaneous characteristics between different disorders in more sensitive and robust way. The effects reported in the present investigation cannot be explained by medication and illness chronicity—two common confounds in psychiatric neuroimaging, since all patients were in their first episode and remained medication-naïve at the time of scanning. Furthermore, all five groups were scanned using the same MRI scanner and image acquisition parameters, therefore our results cannot be explained by systematic differences in the data acquisition. Together, our design, large sample, methodology, and results provide the direct evidence to understand the relationships between subcortical hub pathology and mental disorders.

Limitations and future work

The present study has some potential limitations. First, most of our understanding of subcortical network in clinical neuroscience has come from Magnetic Resonance Imaging (MRI) signal. But subcortical structure is highly heterogeneous and composed of up to many small discrete nuclei (Jones, 2012; de Hollander et al., 2015). Psychiatric symptoms associated with subcortical dysfunction vary based to the location (Salloway and Cummings, 1994). Fine-grained examination of subcortical regions has been limited by the spatial resolution of normal MRI. Moreover, the general analysis protocols including normalization and spatial smoothing may blur the boundaries of multinuclear structures. Future studies may need adopt techniques with ultra-high resolution, such as 7T fMRI, to delineate the role of subcortical network in psychiatric filed. Second, since the current investigation is cross-sectional, we cannot make casual mechanistic inference. One promising approach may need to be considered in future work, which is known as normative modeling, could estimate the extent about how an individual's neural features deviate from what is expected given his/her age. This longitudinal track may provide the casual explanations. Finally,

although we classified different mental disorders by machine learning, and revealed the shared and distinct patterns between different patient population, we did not decipher the relationship between the overlap/similarity on symptoms and similarity on neural patterns.

Conclusion

In conclusion, the current results provide the first evidence that time-varying functional connectivity within subcortical network can effectively show distinct patterns between HC and patients, as well as SZ and OCD, MDD and OCD, SZ and BD, with a large sample size and transdiagnostic approach. Importantly, these main differences came from the functional connections between basal ganglia and thalamus. We are hopeful that our current findings will lead to a refinement to make more precise diagnosis in neuropsychiatry.

Data Availability Statement:

All codes are available at:

https://github.com/psywalkeryanxy/dynamic_FNC_mental_disorders

Reference

1. Goldberg, D. (2015). Psychopathology and classification in psychiatry. *Social psychiatry and psychiatric epidemiology*, *50*(1), 1-5.
2. Clark, L. A., Cuthbert, B., Lewis-Fernández, R., Narrow, W. E., & Reed, G. M. (2017). Three approaches to understanding and classifying mental disorder: ICD-11, DSM-5, and the National Institute of Mental Health's Research Domain Criteria (RDoC). *Psychological Science in the Public Interest*, *18*(2), 72-145.
3. Insel, T. R., & Cuthbert, B. N. (2015). Brain disorders? precisely. *Science*, *348*(6234), 499-500.
4. Fernandes, B. S., Williams, L. M., Steiner, J., Leboyer, M., Carvalho, A. F., & Berk, M. (2017). The new field of 'precision psychiatry'. *BMC medicine*, *15*(1), 1-7.
5. Lewis, G., & Pelosi, A. J. (1990). The case-control study in psychiatry. *Br J Psychiatry*, *157*, 197-207.
6. Sha, Z., Xia, M., Lin, Q., Cao, M., Tang, Y., Xu, K., ... & He, Y. (2018). Meta-connectomic analysis reveals commonly disrupted functional architectures in network modules and connectors across brain disorders. *Cerebral Cortex*, *28*(12), 4179-4194.
7. Parkes, L., Satterthwaite, T. D., & Bassett, D. S. (2020). Towards precise resting-state fMRI biomarkers in psychiatry: synthesizing developments in transdiagnostic research, dimensional models of psychopathology, and normative neurodevelopment. *arXiv preprint arXiv:2006.04728*.
8. Fox, M. D., & Greicius, M. (2010). Clinical applications of resting state functional connectivity. *Frontiers in systems neuroscience*, *4*, 19.
9. Yan, C. G., Chen, X., Li, L., Castellanos, F. X., Bai, T. J., Bo, Q. J., ... & Zang, Y. F. (2019). Reduced default mode network functional connectivity in patients with

recurrent major depressive disorder. *Proceedings of the National Academy of Sciences*, *116*(18), 9078-9083.

10. Baker, J. T., Holmes, A. J., Masters, G. A., Yeo, B. T., Krienen, F., Buckner, R. L., & Öngür, D. (2014). Disruption of cortical association networks in schizophrenia and psychotic bipolar disorder. *JAMA psychiatry*, *71*(2), 109-118.
11. Bell, P. T., & Shine, J. M. (2016). Subcortical contributions to large-scale network communication. *Neuroscience & Biobehavioral Reviews*, *71*, 313-322.
12. Crossley, N. A., Mechelli, A., Scott, J., Carletti, F., Fox, P. T., McGuire, P., & Bullmore, E. T. (2014). The hubs of the human connectome are generally implicated in the anatomy of brain disorders. *Brain*, *137*(8), 2382-2395.
13. Panksepp, J. Affective neuroscience: The foundations of human and animal emotions. Oxford University Press; 1998.
14. Salloway, S., & Cummings, J. (1994). Subcortical disease and neuropsychiatric illness. *The Journal of neuropsychiatry and clinical neurosciences*, *6*(2), 93.
15. Koshiyama, D., Fukunaga, M., Okada, N., Yamashita, F., Yamamori, H., Yasuda, Y., ... & Hashimoto, R. (2018). Role of subcortical structures on cognitive and social function in schizophrenia. *Scientific reports*, *8*(1), 1-9.
16. Schultz, J., Willems, T., Gädeke, M., Chakkour, G., Franke, A., Weber, B., & Hurlemann, R. (2019). A human subcortical network underlying social avoidance revealed by risky economic choices. *Elife*, *8*, e45249.
17. Hibar, D. P., Westlye, L. T., van Erp, T. G., Rasmussen, J., Leonardo, C. D., Faskowitz, J., ... & Andreassen, O. A. (2016). Subcortical volumetric abnormalities in bipolar disorder. *Molecular psychiatry*, *21*(12), 1710-1716.
18. Kong, X. Z., Boedhoe, P. S., Abe, Y., Alonso, P., Ameis, S. H., Arnold, P. D., ... & Francks, C. (2020). Mapping cortical and subcortical asymmetry in obsessive-compulsive disorder: findings from the ENIGMA Consortium. *Biological Psychiatry*, *87*(12), 1022-1034.

19. Schmaal, L., Veltman, D. J., van Erp, T. G., Sämann, P. G., Frodl, T., Jahanshad, N., ... & Hibar, D. P. (2016). Subcortical brain alterations in major depressive disorder: findings from the ENIGMA Major Depressive Disorder working group. *Molecular psychiatry*, *21*(6), 806-812.
20. Gur, R. E., Maany, V., Mozley, P. D., Swanson, C., Bilker, W., & Gur, R. C. (1998). Subcortical MRI volumes in neuroleptic-naive and treated patients with schizophrenia. *American Journal of Psychiatry*, *155*(12), 1711-1717.
21. Man, V., Gruber, J., Glahn, D. C., & Cunningham, W. A. (2019). Altered amygdala circuits underlying valence processing among manic and depressed phases in bipolar adults. *Journal of affective disorders*, *245*, 394-402.
22. Mamah, D., Alpert, K. I., Barch, D. M., Csernansky, J. G., & Wang, L. (2016). Subcortical neuromorphometry in schizophrenia spectrum and bipolar disorders. *NeuroImage: Clinical*, *11*, 276-286.
23. Calhoun, V. D., Miller, R., Pearlson, G., & Adalı, T. (2014). The chronnectome: time-varying connectivity networks as the next frontier in fMRI data discovery. *Neuron*, *84*(2), 262-274.
24. Preti, M. G., Bolton, T. A., & Van De Ville, D. (2017). The dynamic functional connectome: State-of-the-art and perspectives. *Neuroimage*, *160*, 41-54.
25. Liao, X., Cao, M., Xia, M., & He, Y. (2017). Individual differences and time-varying features of modular brain architecture. *Neuroimage*, *152*, 94-107.
26. Liu, J., Liao, X., Xia, M., & He, Y. (2018). Chronnectome fingerprinting: Identifying individuals and predicting higher cognitive functions using dynamic brain connectivity patterns. *Human brain mapping*, *39*(2), 902-915.
27. Fiorenzato, E., Strafella, A. P., Kim, J., Schifano, R., Weis, L., Antonini, A., & Biundo, R. (2019). Dynamic functional connectivity changes associated with dementia in Parkinson's disease. *Brain*, *142*(9), 2860-2872.
28. Damaraju, E., Allen, E.A., Belger, A., Ford, J.M., McEwen, S., Mathalon, D.H., ⋯ Calhoun, V.D., 2014. Dynamic functional connectivity analysis reveals transient

states of dysconnectivity in schizophrenia. Neuroimage 298–308. https://doi.org/10.1016/j. nicl.2014.07.003.

29. Rashid, B., Damaraju, E., Pearlson, G.D., Calhoun, V.D., 2014. Dynamic connectivity states estimated from resting fMRI Identify differences among Schizophrenia, bipolar disorder, and healthy control subjects. Front. Hum. Neurosci. 8, 897. https://doi.org/ 10.3389/fnhum.2014.00897.
30. Wu, X., He, H., Shi, L., Xia, Y., Zuang, K., Feng, Q., ... & Qiu, J. (2019). Personality traits are related with dynamic functional connectivity in major depression disorder: A resting-state analysis. *Journal of Affective Disorders*, *245*, 1032-1042.
31. Reinen, J. M., Chen, O. Y., Hutchison, R. M., Yeo, B. T. T., Anderson, K. M., Sabuncu, M. R., ... Holmes, A. J. (2018). The human cortex possesses a reconfigurable dynamic network architecture that is disrupted in psy- chosis. Nature Communications, 9, 1157.
32. Li, C., Dong, M., Womer, F. Y., Han, S., Yin, Y., Jiang, X., ... & Xu, K. (2020). Transdiagnostic time-varying dysconnectivity across major psychiatric disorders. *Human Brain Mapping*.
33. Allen, E. A., Damaraju, E., Plis, S. M., Erhardt, E. B., Eichele, T., & Calhoun, V. D. (2014). Tracking whole-brain connectivity dynamics in the resting state. *Cerebral cortex*, *24*(3), 663-676.
34. Kim, J. H., Kim, S. Y., Lee, J., Oh, K. J., Kim, Y. B., & Cho, Z. H. (2012). Evaluation of the factor structure of symptoms in patients with schizophrenia. *Psychiatry research*, *197*(3), 285-289.
35. Beck, A. T., & Steer, R. A. (1988). Beck anxiety inventory (BAI). *Überblick über Reliabilitäts-und Validitätsbefunde von klinischen und außerklinischen Selbst-und Fremdbeurteilungsverfahren*, 7.
36. Beck, A. T., Ward, C., Mendelson, M., Mock, J., & Erbaugh, J. (1961). Beck depression inventory (BDI). *Arch Gen Psychiatry*, *4*(6), 561-571.

37. Goodman, W. K., Price, L. H., Rasmussen, S. A., Mazure, C., Fleischmann, R. L., Hill, C. L., ... & Charney, D. S. (1989). The Yale-Brown obsessive compulsive scale: I. Development, use, and reliability. *Archives of general psychiatry*, *46*(11), 1006-1011.
38. Hampson, M., Peterson, B. S., Skudlarski, P., Gatenby, J. C., & Gore, J. C. (2002). Detection of functional connectivity using temporal correlations in MR images. *Human brain mapping*, *15*(4), 247-262.
39. Long, X. Y., Zuo, X. N., Kiviniemi, V., Yang, Y., Zou, Q. H., Zhu, C. Z., ... & Zang, Y. F. (2008). Default mode network as revealed with multiple methods for resting-state functional MRI analysis. *Journal of neuroscience methods*, *171*(2), 349-355.
40. Calhoun, V. D., Adali, T., Pearlson, G. D., & Pekar, J. J. (2001). A method for making group inferences from functional MRI data using independent component analysis. *Human brain mapping*, *14*(3), 140-151.
41. Roweis, S. T. (1998). EM algorithms for PCA and SPCA. In *Advances in neural information processing systems* (pp. 626-632).
42. Abou-Elseoud, A., Starck, T., Remes, J., Nikkinen, J., Tervonen, O., & Kiviniemi, V. (2010). The effect of model order selection in group PICA. *Human brain mapping*, *31*(8), 1207-1216.
43. Bell, A. J., & Sejnowski, T. J. (1995). An information-maximization approach to blind separation and blind deconvolution. *Neural computation*, *7*(6), 1129-1159.
44. Himberg, J., Hyvärinen, A., & Esposito, F. (2004). Validating the independent components of neuroimaging time series via clustering and visualization. *Neuroimage*, *22*(3), 1214-1222.
45. Calhoun VD, Adali T, Pearlson GD, Pekar JJ. Spatial and temporal independent component analysis of functional MRI data containing a pair of task-related waveforms. Hum Brain Mapp 2001b;13: 43– 53.

46. Ystad, M., Eichele, T., Lundervold, A. J., & Lundervold, A. (2010). Subcortical functional connectivity and verbal episodic memory in healthy elderly—a resting state fMRI study. *Neuroimage*, *52*(1), 379-388.
47. Shirer, W. R., Ryali, S., Rykhlevskaia, E., Menon, V., & Greicius, M. D. (2012). Decoding subject-driven cognitive states with whole-brain connectivity patterns. *Cerebral cortex*, *22*(1), 158-165.
48. Varoquaux, G., Gramfort, A., Poline, J. B., & Thirion, B. (2010). Brain covariance selection: better individual functional connectivity models using population prior. *Advances in neural information processing systems*, *23*, 2334-2342.
49. Smith, S. E., Jakobsen, I., Grønlund, M., & Smith, F. A. (2011). Roles of arbuscular mycorrhizas in plant phosphorus nutrition: interactions between pathways of phosphorus uptake in arbuscular mycorrhizal roots have important implications for understanding and manipulating plant phosphorus acquisition. *Plant physiology*, *156*(3), 1050-1057.
50. Friedman, J., Hastie, T., & Tibshirani, R. (2008). Sparse inverse covariance estimation with the graphical lasso. *Biostatistics*, *9*(3), 432-441.
51. Lloyd, S. (1982). Least squares quantization in PCM. *IEEE transactions on information theory*, *28*(2), 129-137.
52. Aggarwal, C. C., & Yu, P. S. (2001, May). Outlier detection for high dimensional data. In *Proceedings of the 2001 ACM SIGMOD international conference on Management of data* (pp. 37-46).
53. Rubinov, M., & Sporns, O. (2010). Complex network measures of brain connectivity: uses and interpretations. *Neuroimage*, *52*(3), 1059-1069.
54. Latora, V., & Marchiori, M. (2001). Efficient behavior of small-world networks. *Physical review letters*, *87*(19), 198701.
55. Zalesky, A., Fornito, A., & Bullmore, E. T. (2010). Network-based statistic: identifying differences in brain networks. *Neuroimage*, *53*(4), 1197-1207.

56. Meyer D., Dimitriadou E., Hornik K., Weingessel A., Leisch F., (2014), e1071: Misc Functions of the Department of Statistics (e1071), TU Wien. R package version 1.6-2, On line at: http://CRAN.Rproject.org/package=e1071.
57. Shi, L., Sun, J., Wu, X., Wei, D., Chen, Q., Yang, W., ... & Qiu, J. (2018). Brain networks of happiness: dynamic functional connectivity among the default, cognitive and salience networks relates to subjective well-being. *Social cognitive and affective neuroscience*, *13*(8), 851-862.
58. Baker, J. T., Dillon, D. G., Patrick, L. M., Roffman, J. L., Brady, R. O., Pizzagalli, D. A., ... & Holmes, A. J. (2019). Functional connectomics of affective and psychotic pathology. *Proceedings of the National Academy of Sciences*, *116*(18), 9050-9059.
59. Pessoa, L. (2016). Beyond disjoint brain networks: overlapping networks for cognition and emotion. *Behavioral and Brain Sciences*, *39*.
60. Furman, D. J., Hamilton, J. P., and Gotlib, I. H. (2011). Frontostriatal functional connectivity in major depressive disorder. *Biol. Mood Anxiety Disord.* 1:11. doi: 10.1186/2045-5380-1-11
61. Van Den Heuvel, M. P., & Sporns, O. (2011). Rich-club organization of the human connectome. *Journal of Neuroscience*, *31*(44), 15775-15786.
62. McColgan, P., Seunarine, K. K., Razi, A., Cole, J. H., Gregory, S., Durr, A., ... & Tabrizi, S. J. (2015). Selective vulnerability of Rich Club brain regions is an organizational principle of structural connectivity loss in Huntington's disease. *Brain*, *138*(11), 3327-3344.
63. Lichtenstein, P., Yip, B. H., Björk, C., Pawitan, Y., Cannon, T. D., Sullivan, P. F., & Hultman, C. M. (2009). Common genetic determinants of schizophrenia and bipolar disorder in Swedish families: a population-based study. *The Lancet*, *373*(9659), 234-239.

64. Gunaydin, L. A., & Kreitzer, A. C. (2016). Cortico–basal ganglia circuit function in psychiatric disease. *Annual review of physiology*, *78*, 327-350.

65. Peters, S. K., Dunlop, K., & Downar, J. (2016). Cortico-striatal-thalamic loop circuits of the salience network: a central pathway in psychiatric disease and treatment. *Frontiers in systems neuroscience*, *10*, 104.

66. Figee, M., Vink, M., de Geus, F., Vulink, N., Veltman, D. J., Westenberg, H., & Denys, D. (2011). Dysfunctional reward circuitry in obsessive-compulsive disorder. *Biological psychiatry*, *69*(9), 867-874.

67. Fallucca, E., MacMaster, F. P., Haddad, J., Easter, P., Dick, R., May, G., ... & Rosenberg, D. R. (2011). Distinguishing between major depressive disorder and obsessive-compulsive disorder in children by measuring regional cortical thickness. *Archives of general psychiatry*, *68*(5), 527-533.

68. Kang, D. H., Kim, S. H., Kim, C. W., Choi, J. S., Jang, J. H., Jung, M. H., ... & Kwon, J. S. (2008). Thalamus surface shape deformity in obsessive-compulsive disorder and schizophrenia. *Neuroreport*, *19*(6), 609-613.

69. Geddes JR, Miklowitz DJ. 2013 Treatment of bipolar disorder. Lancet 381, 1672 – 1682. (doi:10.1016/ S0140-6736(13)60857-0)

70. Jones, E. G. (2012). *The thalamus*. Springer Science & Business Media.

71. de Hollander, G., Keuken, M. C., & Forstmann, B. U. (2015). The subcortical cocktail problem; mixed signals from the subthalamic nucleus and substantia nigra. *PloS one*, *10*(3), e0120572.

Supplemental materials

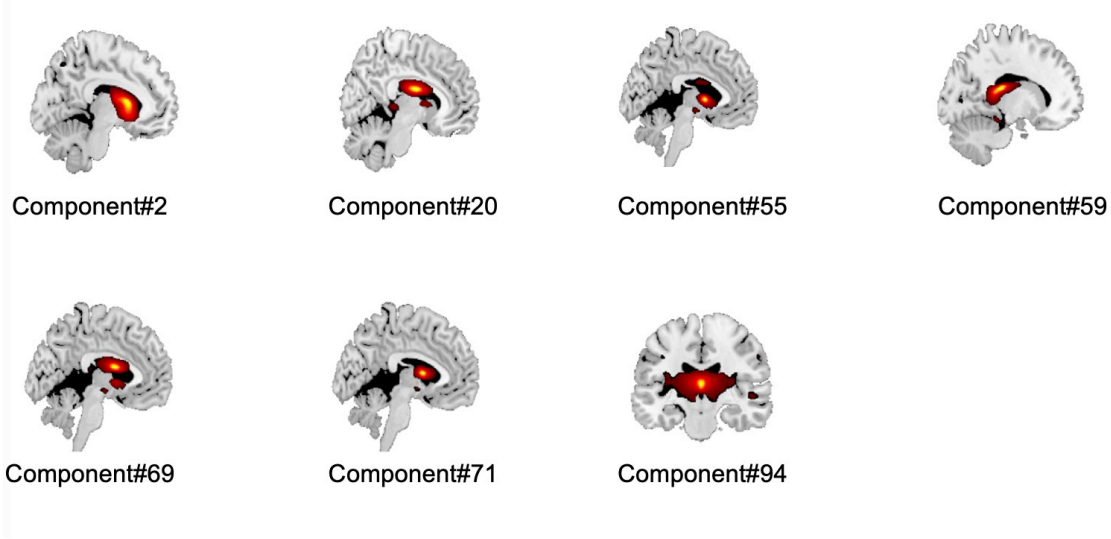

Figure S1. All components in subcortical network.

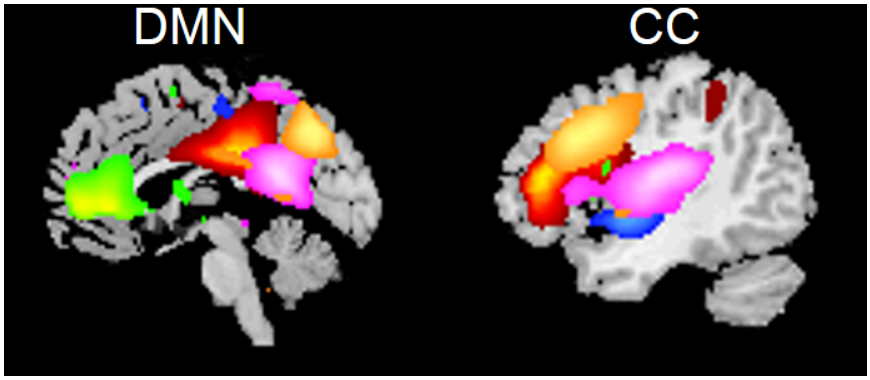

Figure S2. Composite map of the default mode network (DMN) and cognitive control network (CC).

Table S1. Demographic and clinical data from all groups.

Note: BDI, Beck Depression Inventory; BAI, Beck Anxiety Inventory; YMRS, Young Mania Rating Scale; PANSS, Positive and Negative Syndrome Scale.

	Healthy comparison	**Bipolar disorder**	**MDD**	**OCD**	**Schizophrenia**			**Healthy control vs**			
								BD	**MDD**	**OCD**	**SZ**
N	204	49	98	52	142	**F**	**p-value**	**p-values**			
Age	31.119±8.320	33.632±10.280	35.561±10.926	27.365±8.964	26.624±6.055	19.270	<0.001	0.072	<0.001	0.005	<0.001
Age range	17-55	16-58	15-57	12-47	12-58	N/A	N/A	N/A	N/A	N/A	N/A
Gender(female/male)	111/93	23/26	64/34	32/20	72/70	1.862	0.116	0.332	0.077	0.373	0.468
Education	13.930±3.866	10.930±3.460	11.180±3.710	11.060±3.158	11.400±2.921	17.965	<0.001	<0.001	<0.001	<0.001	<0.001
Disease duration(month)	N/A	80.96±92.672	44.54±65.414	50.04±55.613	39.15±44.932	N/A	N/A	N/A	N/A	N/A	N/A
BDI	N/A	9.58±11.349	19.13±7.022	N/A	N/A	N/A	N/A	N/A	N/A	N/A	N/A
BAI	N/A	34.65±13.372	39.18±12.060	N/A	N/A	N/A	N/A	N/A	N/A	N/A	N/A
Y-BOCS (obsessive thoughts)	N/A	N/A	N/A	29.610±8.128	N/A	N/A	N/A	N/A	N/A	N/A	N/A
Y-BOCS (compulsive behaviors)	N/A	N/A	N/A		N/A	N/A	N/A	N/A	N/A	N/A	N/A
PANSS	N/A	N/A	N/A	N/A	82.14±8.977	N/A	N/A	N/A	N/A	N/A	N/A

Table S2. Difference between healthy controls and patients on fraction of time.

HC vs. Patients	F	p-value	η^2	Corrected p-value (FDR, $p<0.05$)
State1	4.413	0.036	0.009	0.048
State2	9.988	0.002	0.020	0.004
State3	1.357	0.245	0.003	0.245
State4	17.938	<0.001	0.035	<0.001

Table S3. Difference among the four groups of patients on fraction of time.

HC vs. Patients		F	p-value	η^2	Corrected p-value (FDR, p<0.05)
State1		0.817	0.486	0.008	0.486
State2		1.655	0.177	0.016	0.354
State3		0.817	0.485	0.008	0.486
State4		5.963	0.001	0.057	0.004
Post hoc analyses for state4	BD vs. MDD	0.787	0.377	0.006	0.377
	BD vs. OCD	1.596	0.210	0.018	0.252
	BD vs. SZ	9.740	0.002	0.058	0.006
	MDD vs. OCD	9.204	0.003	0.063	0.006
	MDD vs. SZ	2.604	0.108	0.012	0.162
	OCD vs. SZ	13.033	<0.001	0.075	<0.001

Table S4. Results of dynamic FNC in default mode network

		HC vs. Patients	F	p-value	η^2	Corrected p-value (FDR, p<0.05)
HC vs. Patients	Mean dwell time	State1	0.006	0.937	<0.001	0.937
		State2	4.448	0.035	0.009	0.070
		State3	5.033	0.025	0.010	0.070
		State4	0.025	0.875	<0.001	0.937
	Fraction of time	State1	0.007	0.932	<0.001	0.932
		State2	4.692	0.031	0.009	0.062
		State3	5.105	0.024	0.010	0.062
		State4	0.019	0.891	<0.001	0.932
	Number of transitions		0.633	0.426	0.001	-
Patients (BD vs. MDD vs. OCD vs. SZ)	Mean dwell time	State1	2.703	0.046	0.026	0.150
		State2	1.374	0.251	0.014	0.334
		State3	0.728	0.536	0.007	0.536
		State4	2.323	0.075	0.023	0.150
	Fraction of time	State1	2.716	0.045	0.027	0.162
		State2	1.393	0.245	0.014	0.326
		State3	0.702	0.552	0.007	0.552
		State4	2.265	0.081	0.022	0.162
	Number of transitions		0.962	0.411	0.010	-

Table S5. Results of dynamic FNC in cognitive control network.

		HC vs. Patients	F	p-value	η^2	Corrected p-value (FDR, p<0.05)
HC vs. Patients	Mean dwell time	State1	1.278	0.259	0.003	0.388
		State2	2.725	0.099	0.005	0.297
		State3	0.052	0.819	<0.001	0.819
		State4	-	-	-	-
	Fraction of time	State1	1.296	0.255	0.003	0.382
		State2	2.808	0.094	0.006	0.282
		State3	0.052	0.819	<0.001	0.819
		State4	-	-	-	-
	Number of transitions		0.097	0.756	<0.001	-
Patients (BD vs. MDD vs. OCD vs. SZ)	Mean dwell time	State1	0.573	0.633	0.006	0.942
		State2	0.551	0.648	0.006	0.942
		State3	0.131	0.942	0.001	0.942
		State4	-	-	-	-
	Fraction of time	State1	0.575	0.632	0.006	0.935
		State2	0.558	0.643	0.006	0.935
		State3	0.142	0.935	0.001	0.935
		State4	-	-	-	-
	Number of transitions		0.230	0.875	0.002	-

Note, no time windows belong to state4, thus there was no statistical results in state 4 within cognitive control network.